



Research article

Concrete stabilization of arsenic-bearing iron sludge generated from an electrochemical arsenic remediation plant

Abhisek Roy^{a,*}, Case M. van Genuchten^b, Indranil Mookherjee^c, Anupam Debsarkar^a, Amit Dutta^a^a Department of Civil Engineering, Jadavpur University, Kolkata 700 032, India^b Department of Earth Sciences – Geochemistry, Utrecht University, Utrecht 3508TA, the Netherlands^c Environment Department, Coal India Limited, Jharkhand 815 351, India

ARTICLE INFO

Keywords:

Arsenic
Concrete
Sustainable sludge management
X-ray absorption spectroscopy

ABSTRACT

In this study, concrete stabilization is adopted to sustainably manage hazardous arsenic-iron sludge near the vicinity of a community-based arsenic water treatment plant for potential use as material for local construction. The strength and workability of the sludge mixed with fresh concrete were investigated to determine the suitability of the concrete mixture for building materials. We found that over 25% sludge (with respect to cement weight) can be incorporated safely into different grades of concrete (M15 and M20). Structural characterization of the concrete mixtures by Fe and As K-edge X-ray absorption spectroscopy indicated a structural transformation of Fe in the sludge from a hydrous ferric oxide to a less ordered phase consistent with Fe siliceous hydrogarnet. Differences in the As K-edge XAS data of samples before and after stabilization in concrete were interpreted as a decrease in As-Fe coordination after concrete stabilization in favor of As-Ca coordination. The leaching of arsenic in the stabilized concrete was examined by the Toxicity Characteristics Leaching Procedure (TCLP) and found to produce < 15 µg/L As, even at the highest sludge mixture fraction (40% sludge with respect to cement weight). The formation of calcite in concrete stabilized arsenic sludge, which was detected by X-ray diffraction (XRD), contributes to the low leachability of arsenic in the sludge for a variety of reasons, including decreasing pore size. In addition, the formation of poorly soluble calcium arsenates can also be responsible for the low mobility of arsenic. Overall concrete stabilization of arsenic-iron sludge can be an effective pre-treatment to safe landfill disposal and, when the arsenic-iron sludge is mixed in specific proportions to achieve desired strength, we propose this concrete can be used locally in nearby construction.

1. Introduction

Arsenic contamination in groundwater is a widespread global water pollution issue that affects most severely communities in the Bengal Basin of India and Bangladesh in South Asia (Fujita et al., 2009; Gadgil et al., 2012; Das and Roy, 2013, 2015; Das et al., 2016; Nazari et al., 2016). The consumption of groundwater containing toxic levels of arsenic increases the risk for various cancers, including skin, lungs and brain (Yoshida et al., 2004; Clancy et al., 2013; Martínez-Cabanas et al., 2015), as well as cardiovascular, respiratory and immune system diseases (WHO, 1996; Yoshida et al., 2004). Arsenic contamination is estimated to affect over 144 million people around the world (Clancy et al., 2013), with over 70 million individuals in South Asia alone (Dhar et al., 1997; Shrestha et al., 2003; Shafiquzzaman et al., 2010). In 1993, the World Health Organization (WHO) adopted a more stringent criterion for arsenic in drinking water by lowering the maximum

permissible limit from 50 to 10 µg/L (WHO, 1996, 2011; USEPA, 2002). This change spurred several countries to adopt the lower limit. However, developing countries like Nepal and Bangladesh retain the previous limit due to technical and economic challenges to achieve 10 µg/L (Das et al., 2009; Clancy et al., 2013; Clancy, 2015).

The arsenic crisis in South Asia has prompted the development and installation of several arsenic removal technologies (Patterson, 2006; Das and Roy, 2015; Das et al., 2016; Liang et al., 2017), many of which rely on sorption of arsenic to oxides of iron (Fe), aluminum (Al) or manganese (Mn) (Martínez-Cabanas et al., 2015). Iron-oxide based sorption technologies, particularly those based on electrolysis of Fe(0) such as Electrochemical Arsenic Remediation (ECAR) (van Genuchten et al., 2012; Amrose et al., 2013a, 2013b; 2014; Das and Roy, 2015; Das et al., 2016) are more efficient and less costly than other sorption technologies and also require less support infrastructure, which facilitates sustainable operation in remote, decentralized communities.

* Corresponding author.

E-mail address: abhisekroy22@gmail.com (A. Roy).<https://doi.org/10.1016/j.jenvman.2018.11.062>

Received 14 May 2018; Received in revised form 14 November 2018; Accepted 15 November 2018

Available online 19 December 2018

0301-4797/ © 2018 Elsevier Ltd. All rights reserved.

Although iron-based treatment technologies are able to remove arsenic to below the WHO recommended level, the resulting arsenic-bearing iron sludge from these technologies can become a new source of arsenic contamination, depending on the redox potential and pH conditions of the long term disposal or storage environments (Banerjee and Chakraborty, 2005). From this perspective, safe disposal or sustainable management of the treated sludge remains one of the most critical and challenging issues facing the sustained operation of Fe-based arsenic treatment systems (Bhunia et al., 2007).

The arsenic-iron sludge produced from Fe-based arsenic treatment cannot be disposed directly in landfills due to the risk of an increase in soil arsenic concentration and groundwater contamination (Ghosh et al., 2004, 2006; Amrose et al., 2013a, 2014). Stabilization processes are often used for many types of waste disposal and have also been recommended for arsenic waste to reduce the mobility of arsenic. These processes include stabilization in cement mortar (Clancy, 2015), lime mortar, brick (Hassan et al., 2014), fly ash and concrete (Banerjee and Chakraborty, 2005). Several researchers observed that the arsenic concentration in the leachate generated from the solidified/stabilized waste during Toxicity Characteristic Leachate Procedure (TCLP) tests (USEPA, 2005) was lower than that generated from non-stabilized waste. While some research has been performed on concrete stabilization of As waste (Jing et al., 2003; Banerjee and Chakraborty, 2005) the results of these studies are not applicable to the present study because of the difference in key properties of the initial sludge, such as water content, elemental composition, quantity and source (laboratory vs existing treatment plant). Furthermore, few studies have evaluated the impact of the amount of incorporated sludge on the variability of the compressive strength of the concrete, and no previous study has focused on the workability of concrete. This part of our study is critical because the concrete stabilized product could be used as construction material if a) the fresh concrete maintains the required workability, b) the hardened concrete has the sufficient standard compressive strength for target structures (e.g. per Indian standard IS 10262:2009 and global standards, such as ACI 318) and c) the arsenic concentration in the leachate generated from demolished concrete cubes during TCLP tests lies within the safe limit. Knowledge of the structural stability, chemical transformation, and arsenic leachability of concrete stabilized arsenic-iron sludge would thus ensure the safe use of concrete in construction near the community-based arsenic treatment plant without significant extra cost, which will encourage the sustainable management of this material locally. Furthermore, even if the sludge concrete mixture fails the desired compressive strength and workability test, concrete stabilization can be a possible pre-treatment before disposal into solid waste sites if arsenic is not found to leach from the mixture.

In this study, our objective is to develop an appropriate method to locally manage hazardous arsenic-iron sludge produced from an existing iron-based arsenic treatment plant by concrete stabilization. We hypothesize that an optimal raw sludge incorporation content exists such that maximum sludge disposal occurs with minimal impact to the strength and arsenic leaching properties of the concrete. To this end, we optimized the amount of sludge that can be mixed into concrete safely, while considering both leachability and compressive strength criteria. Specifically, we a) investigated the workability and compressive strength of different grades of sludge mixed concrete, b) tracked the molecular-scale structural transformations of the arsenic-laden iron oxide sludge in response to stabilization in concrete using synchrotron-based X-ray techniques, and c) evaluated the leaching of arsenic from concrete stabilized waste for different grades of concrete. These results can be used to develop a potential method of local management of treatment residuals in the form of stabilization of arsenic-laden iron oxide sludge in concrete. Thus, the main objective of the study is to develop a cost-effective, locally adoptable, best-practicable and technologically strong method of sludge management.

2. Materials and methods

2.1. Raw material

The arsenic-iron sludge used in this study was obtained from the iron-based Electro Chemical Arsenic Remediation (ECAR) system (Amrose et al., 2014). Sludge samples were collected from two different ECAR plants operated at different locations to consider the variation in sludge characteristics. One of the ECAR plants (600 L per batch capacity) was operated to remediate arsenic from arsenic-spiked synthetic groundwater (natural arsenic concentration = below detectable limit, arsenic concentration after spiking = 350 µg/L) at the Environmental Engineering Laboratory, Department of Civil Engineering, Jadavpur University. The sludge generated from this ECAR plant is hereafter referred to as lab sludge. This plant produced roughly 32 g of dry sludge per 600 L batch (53 mg/L). The other community scale plant was operated to remove arsenic from contaminated groundwater (initial concentration ~ 266 ± 42 µg/L) in Dhapdhapi High School, West Bengal, India. Sludge generated from this community scale ECAR plant is hereafter referred to as field sludge. The community scale plant produced roughly 80 g of dry sludge per 1920 L batch (41 mg/L). Sludge was collected locally from both plants and stored open to the atmosphere prior to use.

Portland Pozzolana Cement (PPC) (Fly Ash Based) of 53 grade conforming to IS (Indian Standard Code of Practice): 1489(Part I):1991 (BIS, 1991) was used in this study and was manufactured by Ambuja Cement. Fine aggregates (i.e. sand) conforming to Zone II (Shah et al., 2006) and stone chips (coarse aggregates) of 20 mm nominal size were used for the preparation of the concrete (BIS, 1970).

Ordinary tap water (pH: 7.8, arsenic: below detectable limit (BDL), chloride: 46 mg/L; sulfate: 10 mg/L, alkalinity: 55 mg/L as CaCO₃) was used for the preparation and curing of concrete cubes. However, deionized (DI) water (resistivity: 18.2 ± 0.3 million ohm-cm) was used for TCLP tests.

2.2. Methods for determination of physical and chemical properties of the raw materials

ECAR field sludge and lab sludge was oven dried at 100–105 °C and powdered to a size less than 500 µm. Both sludges were characterized in terms of optimum moisture content (OMC) and maximum dry density. The OMC and maximum dry density were determined by the light compaction method (IS: 2720 (Part VII-1980)) (BIS, 1980). The unconsolidated undrained triaxial test (BIS, 1993) was used to determine the cohesive property of the sludge samples. The sludge samples were acid digested (USEPA, 1996) for determination of arsenic, iron, and aluminum concentration by Graphite Furnace Atomic Absorption Spectrometry (GFAAS) (Perkin Elmer, AAnalyst 400), with the concentrations of Ca, Mn, and Si determined by Inductively Coupled Plasma Optical Emission Spectrometry (ICP-OES, Perkin Elmer). The concentration of several other parameters, including nitrate (APHA, 1992), phosphate, and available phosphorus (Olsen et al., 1954) were also determined.

2.3. Concrete cube preparation

The dried sludge was mixed in different proportions (i.e. 0%, 5%, 10%, etc. with respect to cement mass) with cement, fine aggregates, coarse aggregates, and water. The sludge amount added replaced an equivalent amount of sand. Extra water corresponding to the OMC of the sludge sample was added to keep the free water-cement (w/c) ratio intact. For moderate exposure conditions and plain cement concrete (PCC) experiments, several trials of mix proportioning were performed following IS 10262:2009 (BIS, 2009) to achieve a characteristic compressive strength of 20 N/mm² i.e. M20 grade of concrete (the letter M refers to the “mix” and the number in the suffix refers to the specified

Table 1
Calculations for mix proportions for preparations of different grade of concrete.

Exposure Condition	Characteristic Compressive strength (f_{ck}) (N/mm ²)	Grade of Concrete	Targeted mean Compressive strength (f'_{ck}) (N/mm ²)	Cement: Fine aggregate: Coarse aggregate (by weight)	Water-cement (w/c) ratio
Moderate	15	M15	20.775	1:2.203:3.495	0.55
Moderate	20	M20	26.600	1:1.920:3.180	0.50
Moderate	25	M25	31.600	1:1.759:3.000	0.47
Moderate	30	M30	38.250	1:1.545:2.714	0.43

characteristic compressive strength after 28 days in N/mm² or MPa). Similarly, for completeness, several trials of mix proportioning were also performed for M15, M25, and M30 grades of concrete, but we focus primarily on the M15 and M20 grades in our study. It is standard practice to ensure the durability of any grade of concrete for a particular exposure condition by limiting the water-cement ratio within the maximum allowable value and maintaining a minimum cement content as per IS 10262:2009 code provisions (BIS, 2009). In the entire course of the present study, the practice of using 'maximum water-cement ratio' and 'minimum cement content' for 'moderate' exposure conditions has been strictly followed to ensure the durability of the concrete on that exposure condition. The calculations of mix proportioning are given in Table 1. These proportions were used while preparing concrete cubes with 0% sludge replacement. In sludge-stabilized concrete cubes, sand was partially replaced by equal weight of sludge. It is worth mentioning that the percentage of sludge replacement was specified with respect to the weight of the cement, but the sludge actually replaces the fine aggregate (sand) in the concrete. Therefore, the cumulative amount of sludge and fine aggregate (or sand) will remain the same for a specific grade.

These proportions of different ingredients were mixed together to prepare fresh concrete. The workability of the fresh concrete mix was determined by the slump cone method. The test was carried out by filling up the slump cone mould (having height of 30 cm, bottom diameter of 20 cm and top diameter of 10 cm) in three equal layers with the mixture being tamped down 25 times for each layer by a 60 mm long steel rod with a 16 mm diameter, which was rounded at one end. After that, the mould was carefully lifted vertically upwards and subsequently the concrete slumps or subsides. The difference in height of the mould and the subsided concrete was measured and termed as vertical settlement or slump height. Slump height, as measured in the slump cone test, indicates the ease of working with the concrete mix. Therefore, a small slump height indicates a low degree of workability. After that, the fresh concrete mix was placed in the cube mould to prepare concrete cubes of dimension 100 mm × 100 mm × 100 mm. The concrete cubes were removed from the mould after 24 h and were placed in water for moist curing. After curing the cubes for 7 and 28 days, the compressive strength of the cubes was also examined. The reaction between cement and water is exothermic by nature. The heat generated by this reaction can create thermal cracks in the concrete cubes, which reduces the durability and strength of the concrete. Curing is a standard practice followed in any concreting work to cool down the concretes which, in turn, minimize the chances of crack formation. Curing of each concrete cube was done in different trays to quantify the arsenic leached from the concrete. The amount of curing water used was 25 L for each cube. The curing water was also tested after 7 and 28 days to determine if any arsenic had leached out of the concrete cubes during curing. We found that the standard errors in replicate measurements of the arsenic concentration in the curing water (CW) by GFAAS was always less than $\pm 0.5 \mu\text{g/L}$, with most below $\pm 0.4 \mu\text{g/L}$. We focus primarily on the M20 and M15 grades of concrete in our study because our goal was to stabilize the arsenic-iron sludge in plain cement concrete (PCC) works having relatively lower compressive strength.

2.4. Solid characterization

2.4.1. X-ray diffraction

Diffraction data was collected to determine the formation of mineral phases in arsenic-iron sludge mixed concrete. XRD patterns of the different concrete cubes were obtained from an X-Pert PRO PANalytical diffractometer with Cu K α radiation ($\lambda = 1.5406 \text{ \AA}$). X-rays were generated with a current of 30 mA and a potential of 45 kV. Scans were performed between 2θ values of 10° and 70° at a scan rate of $0.05^\circ \text{ min}^{-1}$.

2.4.2. X-ray absorption spectroscopy

Samples for XAS analysis were prepared by diluting dried samples of raw sludge and concrete in cellulose to form pellets. For these experiments, we selected only field sludge samples since these samples originate from real world application, rather than the lab sludge samples. In addition, to examine if Fe speciation depended on the size of the pulverized concrete, which would occur if the presence of Fe induced some heterogeneity in the pulverized concrete particles, we investigated two different sized concrete particles: $< 1 \text{ mm}$ and $< 9.5 \text{ mm}$ sieved fractions. These particle cut-offs were based on standard sieve sizes. For the Fe K-edge measurements, the pellet size and the amount of cellulose added was such that the total X-ray absorption from the sample was less than 2.5 absorption lengths, while the absorption of Fe was approximately 1.0 absorption length. Fe K-edge XAS data were collected at the DUBBLE beam line (BM-26) of the European Synchrotron Radiation Facility (ESRF). Spectra were recorded at room temperature out to $k = 13 \text{ \AA}^{-1}$ in transmission mode using ion chambers for measurements of I_0 and I_t . 2 to 4 scans were collected for each sample and a Fe(0) foil was used to calibrate the beam at 7112 eV. As K-edge XAS data were collected at beam line 4-1 of the Stanford Synchrotron Radiation Lightsource (SSRL). 5 to 7 scans were collected for each sample and an Au(0) foil was used to calibrate the beam at 11919 eV. Spectra were recorded at liquid nitrogen temperature in fluorescence mode using a PIPS detector. Spectra of the field sludge were collected out to $k = 13 \text{ \AA}^{-1}$, but because of the dilute As concentration in the concrete sample, spectra were only collected out to $k = 10 \text{ \AA}^{-1}$ due to the low signal-to-noise ratio at high k . Furthermore, the $< 9.5 \text{ mm}$ sieved size sample did not yield usable data presumably due to the larger concrete grains and lack of signal from As. The X-ray beam was detuned 30% (ESRF) or 40% (SSRL) to prevent second-order harmonics. The X-ray absorption near edge structure (XANES) region for both Fe and As data was measured with 0.35 eV steps, whereas step sizes of 0.05 \AA^{-1} were used for the extended X-ray absorption fine structure (EXAFS) region.

Spectra were aligned, averaged, and background-subtracted using SixPack software (Webb, 2005) following standard methods described previously (van Genuchten et al., 2012). The EXAFS spectra were extracted using k^3 -weighting and were Fourier-transformed over the k -range of 2–10.5 or 11 \AA^{-1} with a Kaiser-Bessel window with dk of 3 \AA^{-1} . Analysis of the XANES and EXAFS spectra of the raw field sludge and concrete samples was performed by comparison to the spectra of Fe-bearing and As-bearing reference material. The Fe-bearing references included 2-line ferrihydrite and goethite, whereas the As-bearing references included As(III) and As(V) adsorbed to 2-line ferrihydrite, scorodite ($\text{FeAsO}_4 \cdot 2\text{H}_2\text{O}$), and a calcium arsenate solid. The reference

material synthesis and collection of XAS data for references appears in van Genuchten et al. (2014) (Fe-bearing material) and in van Genuchten et al. (2012) (As-bearing material).

2.5. Methods for leachability testing: TCLP

Leaching characteristics of the sludge mixed concrete were investigated by varying the percentage of sludge mixed for different grades of concrete. In this method, concrete cubes were crushed and passed through a 9.5 mm sieve. 100 g of the crushed and sieved concrete cube materials were used in the TCLP analysis to simulate the conditions pertaining to the end of the service life of the concrete structures containing arsenic-iron sludge. In the TCLP method, 100 g of sample was mixed with 2 L of extraction fluid, which consisted of 0.1 M acetic acid and 0.064 M NaOH at pH 4.95 ± 0.03 . The slurry was mixed using a rotary agitator for 18 h at 30 ± 3 rpm. After mixing, the sample was filtered through a glass microfiber filter paper of pore size $0.7 \mu\text{m}$ (Whatman 1825-047, Grade GF/F). Finally, the solution passing through the filter (i.e. the TCLP leachate) was analyzed for arsenic by GFAAS. While determining the arsenic concentration in leachate produced from the demolished sludge stabilized concrete cubes by TCLP procedure, the standard errors were always less than $\pm 1.2 \mu\text{g/L}$, with most below $\pm 0.3 \mu\text{g/L}$.

3. Results and discussion

3.1. Physical and chemical properties of the sludge

The arsenic-iron sludge, which was produced by co-precipitation of arsenic and ferric (oxyhydr)oxides, was found to have high concentrations of iron (206 ± 14 g/kg, and 87 ± 1 g/kg for lab sludge and field sludge respectively) and arsenic (1219 ± 43 mg/kg and 250 ± 7 mg/kg for lab sludge and field sludge respectively). The fraction of aluminum, which was added as aluminum sulfate for particle aggregation during treatment in both plants, was higher in the lab sludge (92.4 ± 10.2 g/kg) compared to the field sludge (7.3 ± 0.01 mg/kg). For both sludge samples, the arsenic fraction was found to be greater than 50 mg/kg, which classified it as a Class-A type of hazardous waste per Hazardous Material (Management, Handling, and Transboundary Movement) Rules of India, 2008 (MoEF, 2008). The pH value of the sludge was observed to be in the range of 7.65–7.81 for lab sludge and 7.74–8.14 for field sludge, indicating that sludge can be treated as a neutral (or slightly alkaline) material. The OMC content of the dried sludge was found to be $72 \pm 1\%$ and $58 \pm 1\%$ for the lab sludge and field sludge respectively. High OMC values lead to a higher water demand of the sludge, which must be accounted for in addition to the water demand calculated with respect to the water-cement (w/c) ratio. Therefore, an extra amount of water with respect to the OMC of the amount of incorporated sludge was added. The results of the undrained triaxial test suggest that both sludges are cohesionless ($C = 0$) and have a relatively high ϕ (for lab sludge $\phi = 33.3^\circ$ and for field sludge $\phi = 27.5^\circ$). Thus, the sludge behaves like a cohesionless sand particle, which is excellent for replacing sand. The concentration of nitrate, phosphate, and total phosphorus was found to be below the detection limit (BDL) for both sludges. Table 2 shows the results of the physical and chemical characterization of the sludge.

3.2. Compressive strength of different grades of concrete

Various grades of concrete cubes made with different sludge percentages were tested for compressive strength after 7 and 28 days of curing. Fig. 1 presents the compressive strength for different grades of concrete as a function of sludge percentage. We found that increasing the arsenic-iron sludge in the concrete decreased the strength of the cubes. Up to a 30% mix of lab sludge in the M20 grade of concrete reduced the 28 day compressive strength by 38.8%, although it nearly

Table 2

Physical and chemical characterization results of raw sludge.

	Lab Sludge	Field Sludge
Physical Characterization		
OMC (%)	72 ± 1	58 ± 1
Maximum dry density (kg/m^3)	0.883 ± 0.003	1.05 ± 0.01
Chemical Characterization		
pH	7.65–7.81	7.74–8.14
Arsenic (mg/kg)	1219 ± 43	250 ± 7
Iron (g/kg)	206 ± 14	87 ± 1
Aluminium (g/kg)	92.4 ± 10.18	7.3 ± 0.01
Silica (g/kg)	175.1 ± 0.2	229.2 ± 0.2

achieved the targeted compressive strength of 26.6 N/mm^2 . For field sludge, the maximum amount of sludge that can be mixed safely is 27.5%, with an observed reduction of 36.6% in the compressive strength. For the M15 grade of concrete, both sludges can be mixed up to 30% safely, although there was a reduction in strength of 35.3% and 38.6% for lab and field sludge respectively.

3.3. Workability of concrete

The workability of sludge mixed concrete for various grades is shown in Fig. 2. It was observed that the workability of the concrete mix decreased with increasing sludge fraction.

The high OMC value of the sludge (Table 2), which indicates the tendency of the sludge to hold very high moisture, can explain the decrease in workability with increased sludge fraction. An incorporation of 30% by mass of field lab sludge in the M15 grade of concrete mix reduced the slump height from 40 mm to 15 mm, whereas for incorporation of the same amount of field sludge, a 20 mm decrease was observed. For the M20 grade of concrete, 30% addition of lab sludge resulted in a decrease of workability from 35 mm to 10 mm, whereas addition of 27.5% field sludge led to a reduction of workability from 35 mm to 20 mm.

It was also observed that the average weight of the arsenic-iron mixed concrete cubes decreased with increasing percentage of sludge. This observation suggests that for equal volume of cubes (1000 cm^3), the sludge has a lower density (or higher water content) compared to the other ingredients of the concrete mix.

3.4. Structural transformation of arsenic-iron sludge induced by concrete stabilization

3.4.1. Changes in Fe speciation

The Fe K-edge XANES and EXAFS spectra of the arsenic-iron field sludge samples before and after stabilization in concrete (grade M20) are compared to reference spectra in Fig. 3. In this figure, two concrete samples are given, which have been separated by size ($< 1 \text{ mm}$ and $< 9.5 \text{ mm}$ fractions). The XANES spectra and first derivatives (Fig. 3A and B) of the raw field sludge closely matched the goethite and ferrihydrite references, which indicates that the field sludge consists of primarily trivalent Fe. The XANES spectra of both concrete samples ($< 1 \text{ mm}$ and $< 9.5 \text{ mm}$ fractions) are virtually identical, which indicates that Fe speciation in the concrete does not depend on concrete particle size, but both concrete samples differ relative to the raw field sludge and ferrihydrite. These differences imply a modification in the Fe coordination environment of the field sludge induced by mixing in concrete. As highlighted by the arrow in the XANES derivative spectra (Fig. 3B), the concrete samples have a shoulder with higher intensity than the field sludge and ferrihydrite samples near 7120 eV.

Similar to the XANES spectra, the EXAFS spectrum of the field sludge matches that of ferrihydrite, including the first symmetric oscillation from 3.5 to 5 \AA^{-1} , a distinct peak centered near 7.5 \AA^{-1} , and the broad oscillations at $k > 9 \text{ \AA}^{-1}$. By contrast, the EXAFS spectra of

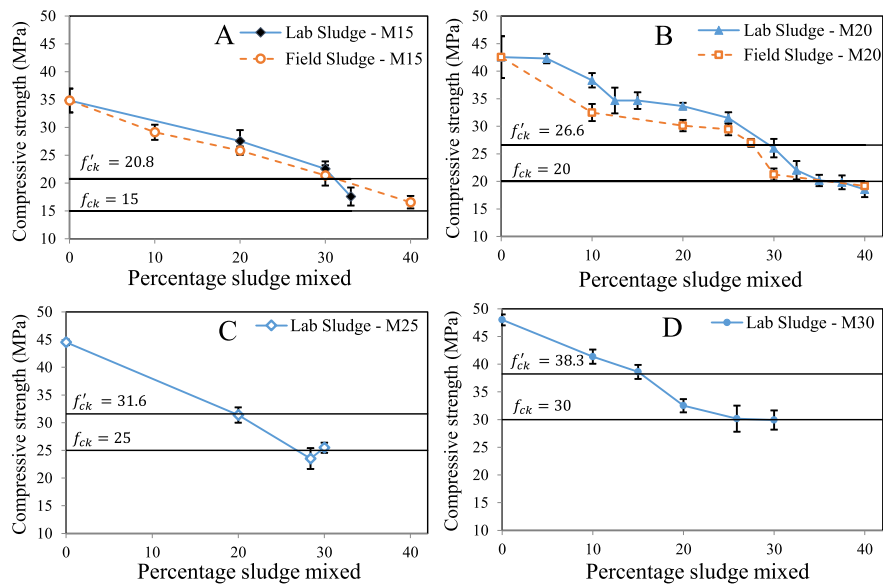


Fig. 1. Compressive strength (N/mm^2) of concrete cubes after 28 days of curing as a function of percentage sludge mixed. A) Field sludge-M15 and Lab sludge -M15, B) Field sludge-M20 and Lab sludge -M20, C) Lab sludge -M25, and D) Lab sludge -M30. The horizontal solid lines represent the desired characteristic compressive strength (f'_{ck}) and the Targeted mean Compressive strength (f'_{ck}). Lines connecting each data point serve only to guide the eye.

the concrete samples show several differences in line shape relative to the EXAFS spectrum of ferrihydrite and goethite. As shown by the arrows in Fig. 3C, the concrete samples are characterized by an asymmetric first oscillation from 3.5 to 5 \AA^{-1} and the presence of a shoulder at lower k in the peak centered at 6 \AA^{-1} . In addition, the clear peak at 7.5 \AA^{-1} appearing in the field sludge sample shifts to higher k and forms a shoulder with the adjacent oscillation in the concrete samples. These features in the EXAFS spectra of the concrete samples are remarkably similar to previously reported Fe K-edge EXAFS spectra of Fe-bearing phases in cement, particularly Fe siliceous hydrogarnet (Dilnesa et al., 2014; Vespa et al., 2015), and synthetic Fe-ettringite (Möschner et al., 2008).

The differences in the EXAFS spectra of the concrete samples relative to the field sludge, ferrihydrite, and goethite are manifest in the Fourier-transformed EXAFS spectrum (Fig. 3D) primarily in the second-shell peak position and amplitude. The second-shell peaks of the field sludge and ferrihydrite (dashed vertical line in Fig. 3D) samples are similar in position and amplitude, suggesting a similar nanoscale structure that is less ordered than goethite. The second-shell peaks of the field sludge and ferrihydrite samples are characterized by a peak centered near 2.8 \AA ($R + \Delta R$), with a subtle shoulder at increasing R , which indicates the presence of both edge- and corner-sharing FeO_6 octahedra (Manceau and Fourier, 1993). By contrast, the second-shell peak amplitude is highly reduced in the concrete samples, and the peak maximum is located at $R + \Delta R$ above 3.0 \AA . Although the concrete mixture used in our study contained some native Fe-bearing material

(tricalcium alumino ferrite), the amount of Fe sludge added to the mixture far outweighed the native Fe fraction of the concrete. Therefore, these strong second-shell differences for the concrete samples relative to the raw field sludge and Fe-bearing references suggest that the arsenic-iron field sludge has undergone a structural transformation following mixing in concrete, in which nearly all edge- and corner-sharing Fe-Fe bonds have been broken. Considering the unique chemistry of cement mixtures (i.e. high pH, high concentrations of Ca, Si), it is not surprising that the structure of the arsenic-iron sludge was not maintained. The position and amplitude of the second-shell peak suggest that Fe in the concrete mixture is not speciated as a Fe(III) precipitate, but is coordinated to a weakly scattering element that connects with Fe polyhedra to form relatively long bonds, such as Ca. In support of this result, the stable Fe-bearing phases reported to form in cement mixtures, which bear similar second-shell peaks to the concrete samples in our study (Dilnesa et al., 2014; Vespa et al., 2015) have been shown to lack Fe-Fe bonds in favor of longer Fe-Ca polyhedral connections (Vespa et al., 2015). Therefore, we conclude that the arsenic-iron sludge has transformed from a ferrihydrite-like Fe(III) precipitate in the raw sludge to a solid similar to Fe siliceous hydrogarnet, in which Fe polyhedra link primarily with Ca.

3.4.2. Changes in As speciation

The As K-edge XANES and EXAFS spectra of the field sludge and concrete samples are given alongside those of As(III) and As(V)-bearing reference materials in Fig. 4. The absorption maximum in the XANES

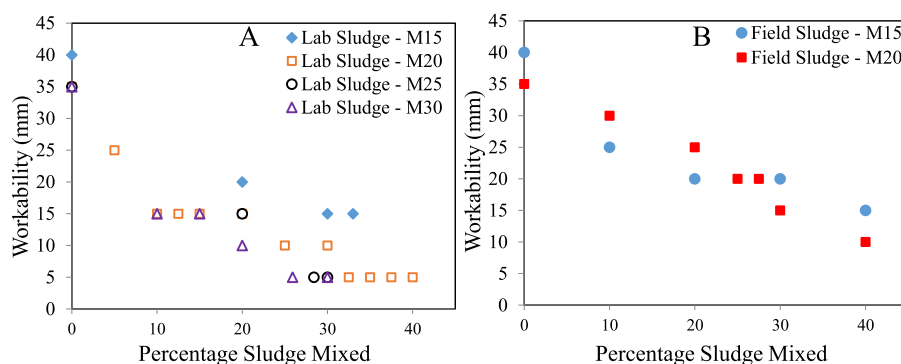


Fig. 2. Workability (mm) for different grades of concrete as a function of percentage sludge mixed. A) Lab sludge -M15, Lab sludge -M20, Lab sludge -M25, and Lab sludge -M30, B) Field sludge-M15 and Field sludge-M20.

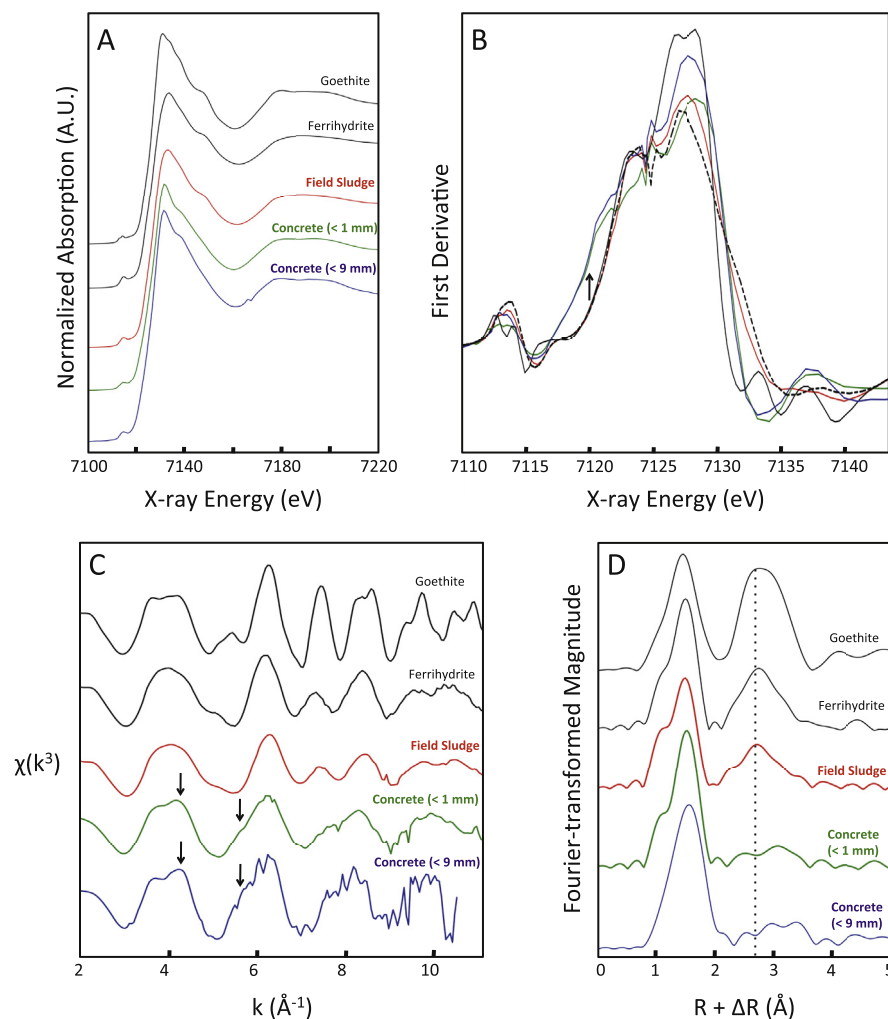


Fig. 3. Fe K-edge XANES and EXAFS spectra of the field sludge before and after stabilization in M20 grade of concrete. A) XANES spectra, B) first derivative XANES spectra, C) EXAFS spectra, and D) Fourier-transformed EXAFS spectra. The field sludge sample appears in red, whereas the concrete samples appear in green (< 1 mm fraction) and blue (< 9.5 mm fraction). XAS data of Fe-bearing reference minerals are shown in black, with the dashed line in B) representing ferrihydrite and the solid line representing goethite. The arrows in B and C highlight structural changes induced by incorporation into concrete. The vertical dashed line in D highlights the contribution of edge-sharing Fe octahedra to the second-shell of the Fourier-transformed EXAFS spectra for goethite, ferrihydrite, and the field sludge. (For interpretation of the references to colour in this figure legend, the reader is referred to the Web version of this article.)

spectra for both field sludge and concrete samples matches that of the As(V) references, which indicates that As is present primarily as As(V) in the samples. However, subtle differences between the XANES spectra of the sludge and concrete samples are apparent. The overlay of the raw sludge and concrete XANES spectra in Fig. 4B reveals a small shoulder in the raw sludge near 11870 eV, which indicates the presence of a minor fraction of As(III) in the raw sludge. In addition, the overlay of the XANES spectra also indicates a difference in the post-edge region, particularly the first oscillation after the absorption edge. The dashed vertical line in Fig. 4B highlights the greater intensity in the oscillation centered near 11891 eV for the concrete sample relative to the raw sludge. This intensity and position matches closely a post-edge feature in the XANES spectrum of the calcium arsenate reference.

Differences in the EXAFS spectra of the field sludge and concrete samples relative to the reference EXAFS spectra in Fig. 4C show that the samples are not a good match to scorodite, an As(V)-bearing Fe mineral, or As(III) adsorbed to Fh. The closest match to the EXAFS spectrum of the field sludge was that of the As(V) adsorbed to Fh (As(V) Ads Fh) reference. Indeed, the EXAFS spectra overlays in Fig. 4D show that the line shape and phase of the EXAFS oscillations of the field sludge sample matched almost identically with those of As(V) Ads Fh, including the small asymmetrical shoulders in the first two oscillations centered at 4.5 and 7.5 Å⁻¹. Because As(V) binds to Fh primarily in double corner-sharing binuclear geometries (Waychunas et al., 1993; van Genuchten and Peña, 2016), the nearly identical match of the field sludge EXAFS spectrum indicates that As in the field sludge is bound in similar inner-sphere complexes to Fe(III) oxides in the raw sludge.

The first two oscillations of the EXAFS spectrum of the concrete sample differ relative to those of the field sludge and As(V) Ads Fh, which suggests a change in As(V) speciation upon stabilization in concrete. In particular, the first EXAFS oscillation centered near 4.5 Å⁻¹ in the concrete sample is symmetric (see arrows in Fig. 4C), which contrasts the broadened and asymmetric first oscillation in the field sludge, but is similar to that of the calcium arsenate reference. In a previous study that examined As speciation in samples produced by mixing As-bearing Fe oxides with cement, Jing et al. (2003) present EXAFS spectra with a similar symmetric shape of the oscillation near 4.5 Å⁻¹ and conclude that direct As-Ca coordination occurred after mixing. The broadening and asymmetry of the first oscillation in EXAFS spectra of As(V)-bearing solids, which occurs in the field sludge sample, has been attributed to the interference between As-O and As-Fe atomic pairs (Paktunc et al., 2008). Consequently, the symmetric oscillation at 4.5 Å⁻¹ in the concrete sample suggests decreased As-Fe coordination in the concrete sample. The EXAFS overlays of the concrete sample in Fig. 4D reveal that the calcium arsenate reference is a better match to the symmetric first oscillation than As(V) Ads Fh, but a poorer match to other EXAFS features (indicated by the * symbol). Therefore, while it is not possible to determine the exact As coordination environment in the concrete sample with the As K-edge XAS data alone, combining the Fe oxide transformations revealed by the Fe K-edge XAS analysis with the subtle and systematic changes in the As K-edge XAS data suggests a decrease in As-Fe coordination following concrete stabilization in favor of As-Ca coordination.

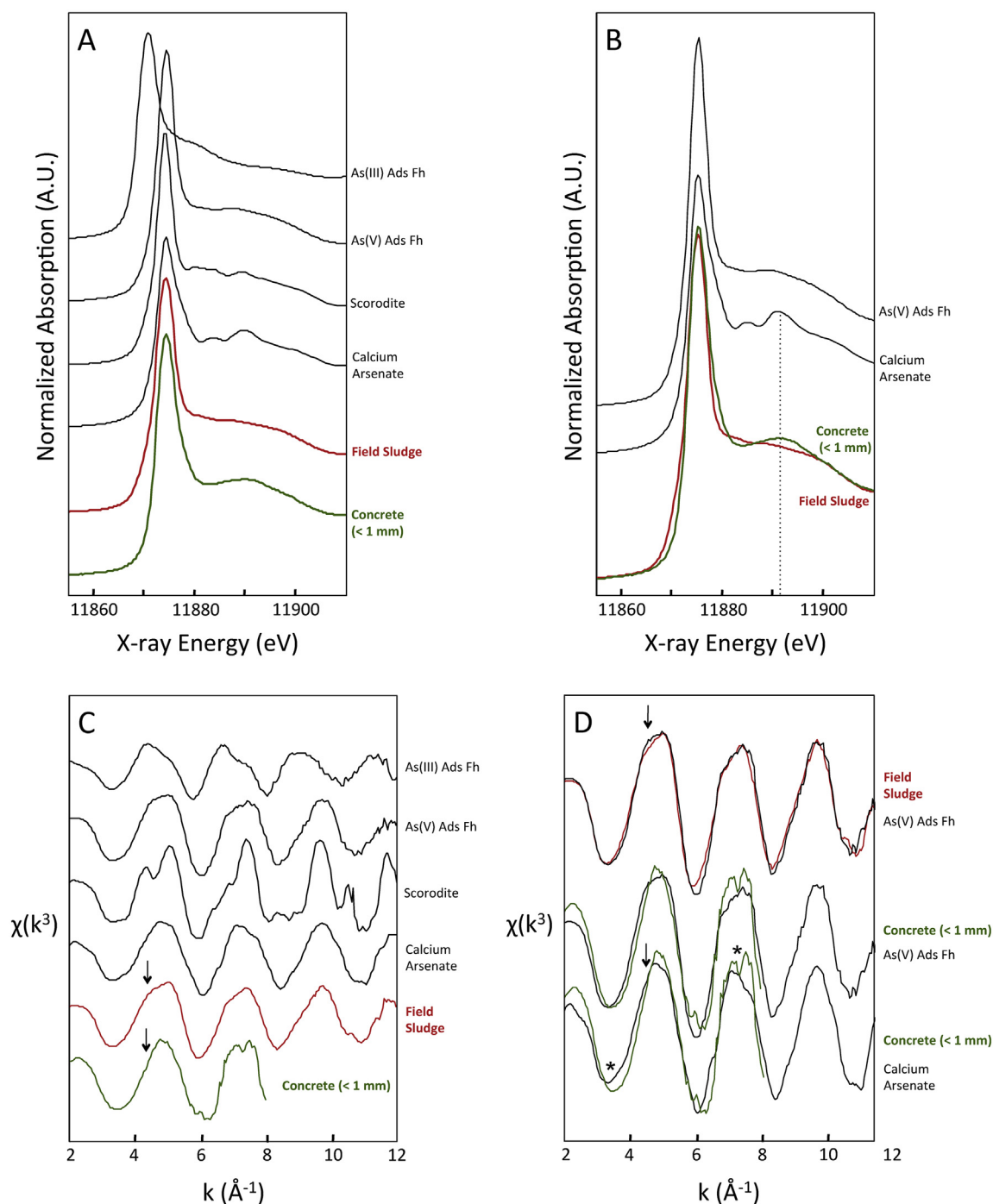


Fig. 4. As K-edge XANES and EXAFS spectra of the field sludge before and after stabilization in M20 grade of concrete. A) XANES spectra, B) overlay of field sludge and concrete, C) EXAFS spectra, and D) overlay of EXAFS spectra of raw sludge and concrete samples with reference material. The field sludge sample appears in red, whereas the concrete sample appear in green (< 1 mm fraction). The dashed vertical line in B indicates a change in the post-edge XANES region upon stabilization in concrete. The arrows in C and D highlight changes in the EXAFS spectra due to stabilization in concrete. (For interpretation of the references to colour in this figure legend, the reader is referred to the Web version of this article.)

3.5. Leachability of concrete

Fig. 5 shows the variation of leached arsenic concentrations ($\mu\text{g/L}$) in 25 L of curing water (CW) after a curing period of 7 and 28 days. The test results indicate that the concentration of leached arsenic in curing water was very low, and in all cases, was less than $2 \mu\text{g/L}$. This low arsenic concentration in the leached CW is far below the disposable standard of treated leachate ($< 5000 \mu\text{g/L}$) (Ministry of Environment, Forest and Climate Change, MoEFCC, 2016). Although CW is not an

aggressive leaching solution, the low arsenic concentration in the leached CW points to the stability of arsenic in the concrete mixture.

Fig. 6 shows the changes in arsenic concentration in the TCLP leachate at $\text{pH } 4.93 \pm 0.03$, which contained 0.1 M acetic acid and 0.064 M NaOH. In this figure, we plot the concentration of As in TCLP leachate as a function of different grades of concrete at different sludge fractions (dry sludge mix up to 40% with respect to dry cement weight). From Fig. 6 it is observed that, in almost all the grades of concrete, the concentration of arsenic in the produced leachate increased with

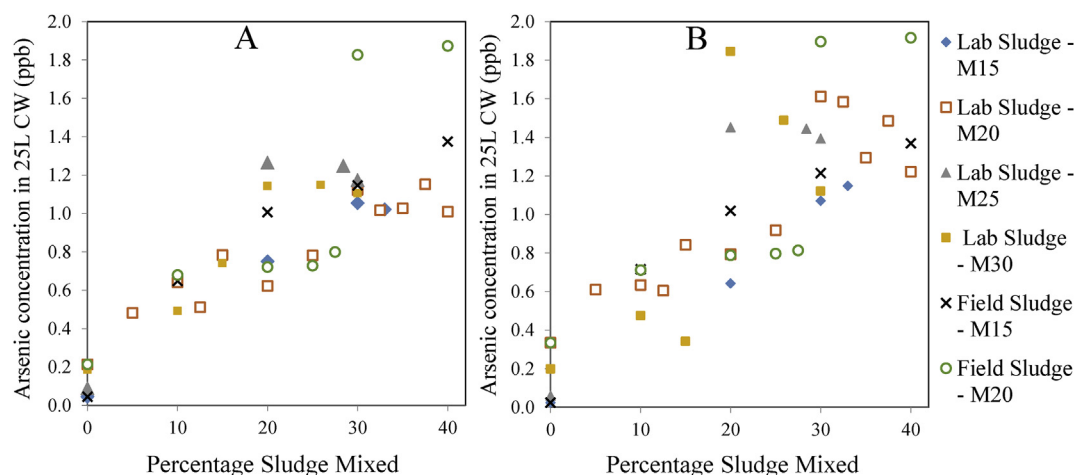


Fig. 5. Variation of Arsenic concentration ($\mu\text{g/L}$) in the curing water with the percentage of sludge mixed in the concrete. A) 7 day cured cubes and B) 28 day cured cubes.

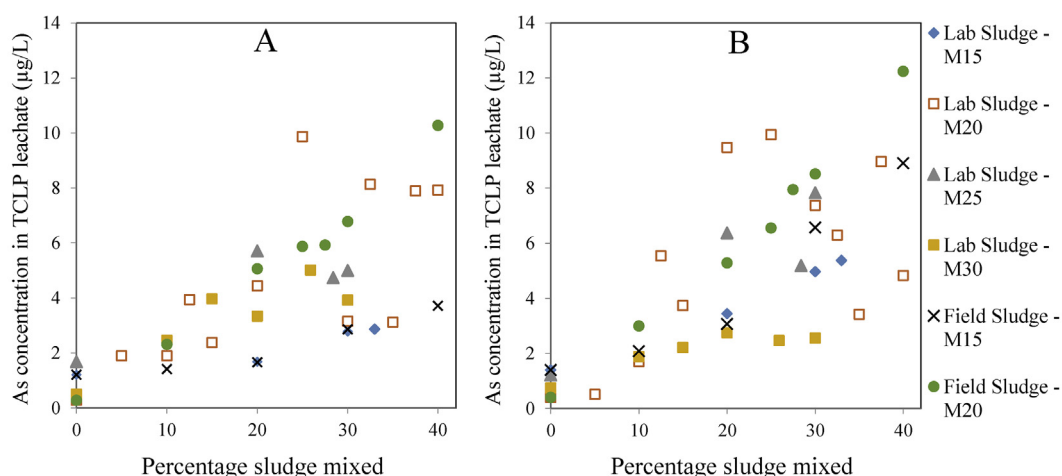


Fig. 6. Variation of arsenic concentration ($\mu\text{g/L}$) in leachate (by TCLP method) with the percentage of sludge mixed in concrete. A) 7 day cured cubes and B) 28 day cured cubes.

increasing percentages of sludge for both curing options (i.e. curing for 7 or 28 days).

It was also observed that the concentrations of arsenic in the leachate for all grades of concrete and both curing options were substantially less than the safe discharge standard of $200 \mu\text{g/L}$ (the safe disposal limit of arsenic in treated leachate). Furthermore, in all cases, the observed arsenic concentration in the leachate was even below $20 \mu\text{g/L}$.

3.6. Factors contributing to sludge stabilization in concrete

In Fig. 7, we present the percentage of total leached arsenic (in CW and TCLP leachate), which was calculated by considering the average concentration of arsenic in the dry sludge, the average weight of the concrete cubes, and the amount of sludge used for the preparation of the concrete cubes. Fig. 7 shows that for all the grades of concrete the total leached arsenic concentration was less than 2%. This arsenic concentration measured in the CW and in the leachate is extremely low, which indicates that arsenic has been sufficiently stabilized in concrete. In the following paragraphs, we discuss a number of possible factors for the observed stabilization of arsenic.

Factor-I: Cement is a heterogeneous mixture of quick lime (CaO or C), silica (SiO_2 or S), alumina (Al_2O_3 or A), and iron oxide (Fe_2O_3 or F). The Portland slag cement (PSC) used for the concrete work was a

mixture of four Bogue's compounds: i) Tricalcium silicate (C_3S), ii) Dicalcium silicate (C_2S), iii) Tricalcium aluminate (C_3A), and iv) Tetracalcium aluminoferrite (C_4AF). During the concreting process these Bogue's compounds present in cement are mixed with water, with C_3S and C_2S reacting with water to form calcium silicate hydrate (or C-S-H) gel and hydrated lime ($\text{Ca}(\text{OH})_2$). Carbon dioxide (CO_2) present in the atmosphere, penetrates through the structures and reacts in the presence of water with hydrated lime ($\text{Ca}(\text{OH})_2$) to form calcium carbonate (CaCO_3), which was subsequently confirmed by XRD. This calcium carbonate can block the pores of the concrete, which decreases the effective surface area susceptible to reacting with the leachant and thus reduces the mobility of arsenic (Singh and Pant, 2006).

Factor-II: According to Stronach et al. (1997), Vandecasteele et al. (2002) and Glasser (1997), the formation of poorly soluble calcium arsenates (e.g. $\text{Ca}_3(\text{AsO}_4)_2$) may lead to lower mobility of arsenic in the leachate and CW. Although we were unable to determine the exact As coordination environment following mixture in concrete, partly because the dilute As concentration in the concrete prevented the collection of high quality As K-edge EXAFS at high k , this explanation is consistent with our XAS data set. In Section 3.4, we observed that the structure of arsenic-iron sludge transformed into a solid similar to Fe siliceous hydrogarnet. Because arsenic is taken up initially by the iron sludge presumably in corner-sharing (^2C) binuclear coordination geometries (van Genuchten et al., 2014, 2012), which require edge-sharing

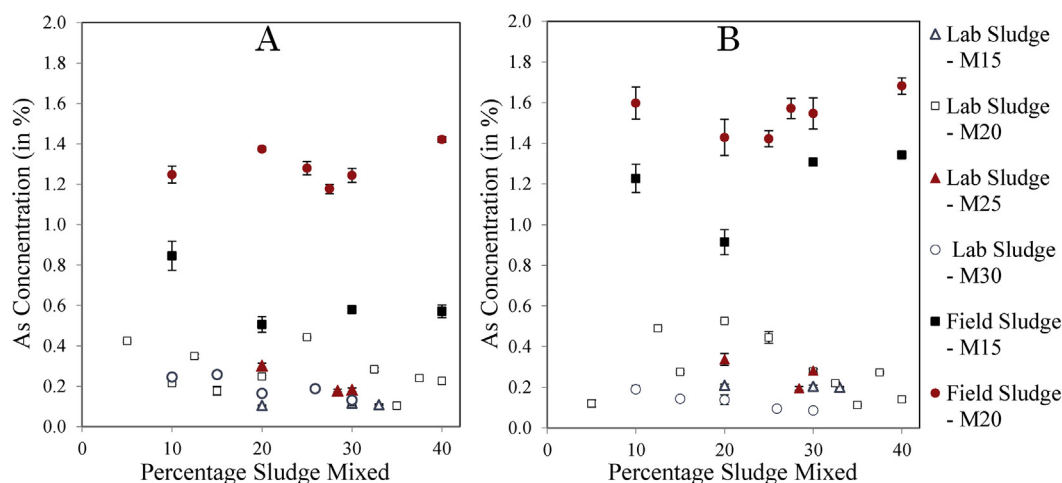


Fig. 7. Graph of total arsenic leached (CW + Leachate, in %) as a function of percentage sludge mixed average. A) 7 day cured cubes and B) 28 day cured cubes.

Fe polyhedra, the absence of Fe-Fe linkages in the concrete mixture suggests that arsenic no longer binds to Fe in this geometry. In addition, the symmetric shape of the first oscillations of the As K-edge EXAFS of the concrete stabilized sample suggests a decreased presence of Fe-As atomic pairs. Based on the high pH and high Ca concentration of cement, which favors calcium arsenate formation, it is likely that arsenic is not bound in binuclear corner-sharing geometries to the Fe(III) precipitates, but has formed a separate Ca- and As-bearing solid. This explanation is supported by previous work investigating the fate of arsenic in cement (Jing et al., 2003).

Factor-III: Hydrated lime and calcium-silicate-hydrate make the concrete matrix alkaline and provide some buffering capacity, which prevents the mildly acidic leaching solution from dissolving the arsenic-bearing solid phase and therefore leads to stabilization of arsenic in the concrete matrix (Dermatas et al., 2004).

3.7. Field recommendations

Based on our results and analyses, we conclude that the quality of the sludge mixed concrete (i.e. compressive strength and workability) depends strongly on the amount of the sludge mixed and the (w/c) ratio. The w/c ratio is the critical parameter that must be optimized first to obtain the desired compressive strength without hindering the workability. Once this information is known, the amount of the sludge should be optimized to immobilize the arsenic in concrete without hindering the desired workability.

It was observed that the concentration of arsenic in the produced leachate and curing water was within the safe discharge limit even up to 40% sludge (w.r.t. cement weight) mixed with M15 and M20 concrete. Furthermore, sludge replacement in the higher grades of concrete (i.e. M25 and M30) produced leachate with extremely low concentrations of arsenic. However, we recommend the use of sludge only in M15 and M20 grades, which can be used for lower strength structures instead of M25 and M30 grades used in superstructures that require high strength. Based on these results, we propose that sludge mixed concrete can be utilized for the construction of low strength structures in the vicinity of the plant.

4. Conclusions

In this work, we demonstrated a socio-economically feasible and technically robust strategy for the management of hazardous arsenic-iron sludge. The compressive strength and workability of the concrete, along with various other parameters, was measured with varying amounts of arsenic-iron sludge in the concrete mixture. The study was performed with different grades of concrete, and also with two types of

sludge (synthetic sludge and sludge obtained from an existing arsenic treatment plant), which ensures the robustness of our results. In every case, the concentration of arsenic in the leachate was well below the safe discharge limit of 5000 µg/L.

Laboratory results of TCLP testing highlight the fact that the hazardous arsenic-iron sludge (with high arsenic and iron content) can be stabilized in the concrete, which we suspect is due to the formation of less soluble calcium arsenates formed following the cement-induced structural transformation of the arsenic-iron sludge. With respect to the utilization of the sludge in construction grade concrete, the key findings of this study are: i) 30% of sludge (w.r.t. cement weight) can be mixed safely in the case of the M15 grade of concrete, ii) 27.5% of sludge (w.r.t. cement weight) can be incorporated safely in the case of the M20 grade of concrete w.r.t the compressive strength, and iii) after adopting a suitable factor of safety, the recommended percentage of sludge that can be mixed safely is 20%.

Acknowledgments

This work was supported by the USAID-DIL (Grant No: 0008660, 2015), IUSSTF, UGC UPE-II and NWO Veni Grant (Project No. 14400). The Authors would like to thank Professor Ashok Gadgil (University of California Berkley) for his long term association with the team, where he provided scientific and engineering advice and ECAR technology deployment and constant encouragement to take up the current research. We acknowledge discussions with Dr. Susan Amrose (until 2016 at UC Berkeley, and now at Massachusetts Institute of Technology) and Prof. Joyashree Roy (Professor of Economics, Jadavpur University) and acknowledge their valuable suggestions during the progress of this research. The authors acknowledge assistance from Mr. Rajesh Bhattacharya, Mr. Surajit Bhandari, and Mr. Sanjib Kumar Paul during field and laboratory work. Dipanjan Banerjee at the Dutch-Belgium beam line of ESRF is thanked for support during the collection of EXAFS spectra.

Appendix A. Supplementary data

Supplementary data to this article can be found online at <https://doi.org/10.1016/j.jenvman.2018.11.062>.

References

- Amrose, S.E., Bandaru, S.R.S., Delaire, C., van Genuchten, C.M., Dutta, A., DebSarkar, A., Orr, C., Roy, J., Das, A., Gadgil, A.J., 2014. Electro-chemical arsenic remediation: Field trials in West Bengal. *Sci. Total Environ.* 488–489, 539–546. <https://doi.org/10.1016/j.scitotenv.2013.11.074>.

- Amrose, S.E., Gadgil, A., Srinivasan, V., Kowolik, K., Muller, M., Huang, J., Kostecki, R., 2013a. Arsenic removal from groundwater using iron electrocoagulation: Effect of charge dosage rate. *J. Environ. Sci. Heal. Part A Toxic/Hazard. Subst. Environ. Eng.* 48, 1019–1030. <https://doi.org/10.1080/10934529.2013.773215>.
- Amrose, S.E., Gadgil, A.J., Bandaru, S.R.S., Delaire, C., van Genuchten, C.M., Li, L., Orr, C., Dutta, A., Debsarkar, A., Das, A., Roy, J., 2013b. Locally affordable and scalable arsenic remediation for South Asia using ECAR. In: 36th WEDC International Conference: Delivering Water, Sanitation and Hygiene Services in an Uncertain Environment, pp. 6.
- APHA, 1992. 18th Ed. Standard Methods for the Examination of Water and Wastewater. Stand. Methods Exam. Water Wastewaters, vol. 552 Am. Public Heal. Assoc., Washingt. 4-87-4-88.
- Banerjee, G., Chakraborty, R., 2005. Management of arsenic-laden water plant sludge by stabilization. *Clean Technol. Environ. Policy* 7, 270–278. <https://doi.org/10.1007/s10098-005-0275-1>.
- Bhunia, P., Pal, A., Bandyopadhyay, M., 2007. Assessing arsenic leachability from pulverized cement concrete produced from arsenic-laden solid CalSiCo-sludge. *J. Hazard. Mater.* 141, 826–833. <https://doi.org/10.1016/j.jhazmat.2006.07.055>.
- BIS, 2009. Concrete Mix Proportioning - Guidelines. Bur. Indian Stand. IS 102622009.
- BIS, 1993. Determination of the shear strength parameters of a specimen tested in Unconsolidated Undrained triaxial compression without the measurement of pore water pressure. Bur. Indian Stand. (BIS), IS.2720-11.
- BIS, 1991. Portland pozzolana cement-specification. Bur. Indian Stand. IS 1489 (Part 1).
- BIS, 1980. Determination of water content-dry density relation using light compaction. Bur. Indian Stand. (BIS), IS.2720-2727.
- BIS, 1970. Specification for Coarse and Fine Aggregate From Natural Sources for Concrete. Bur. Indian Stand. (BIS) IS 383 (Second rev.).
- Clancy, T.M., 2015. Biogeochemical evaluation of disposal options for arsenic-bearing wastes generated during drinking water treatment by. Ph.D. Diss.. Univ. Michigan.
- Clancy, T.M., Hayes, K.F., Raskin, L., 2013. Arsenic waste management: A critical review of testing and disposal of arsenic-bearing solid wastes generated during arsenic removal from drinking water. *Environ. Sci. Technol.* 47, 10799–10812. <https://doi.org/10.1021/es401749b>.
- Das, A., Roy, J., 2015. Jole Arsenic: Prasanga Paschim Banga. Mitram, Kolkata.
- Das, A., Roy, J., 2013. Socio-economic fallout of Arsenicosis in West Bengal: a case study in Murshidabad district. *J. Indian Soc. Agric. Stat.* 67, 267–278.
- Das, A., Roy, J., Chakraborti, S., 2016. Socio-Economic Analysis of Arsenic Contamination of Groundwater in West Bengal, India Studies in Business and Economics. Springer Singapore, Singapore. <https://doi.org/10.1007/978-981-10-0682-1>.
- Das, B., Rahman, M.M., Nayak, B., Pal, A., Chowdhury, U.K., Mukherjee, S.C., Saha, K.C., Pati, S., Quamruzzaman, Q., Chakraborti, D., 2009. Groundwater Arsenic Contamination, Its Health Effects and Approach for Mitigation in West Bengal, India and Bangladesh. *Water Qual. Expo. Heal.* 1, 5–21. <https://doi.org/10.1007/s12403-008-0002-3>.
- Dermatas, D., Moon, D.H., Menounou, N., Meng, X., Hires, R., 2004. An evaluation of arsenic release from monolithic solids using a modified semi-dynamic leaching test. *J. Hazard. Mater.* 116, 25–38. <https://doi.org/10.1016/j.jhazmat.2004.04.023>.
- Dhar, R.K., Biswas, B.K., Samanta, G., Mandal, B.K., Chakraborti, D., Roy, S., Jafar, A., Islam, A., Ara, G., Kabir, S., Khan, A.W., Ahmed, S.A., Hadi, S.A., 1997. Groundwater arsenic calamity in Bangladesh. *Curr. Sci.* 73, 48–59.
- Dilnesa, B.Z., Wieland, E., Lothenbach, B., Dähn, R., Scrivener, K.L., 2014. Fe-containing phases in hydrated cements. *Cement Concr. Res.* 58, 45–55. <https://doi.org/10.1016/j.cemconres.2013.12.012>.
- Fujita, T., Taguchi, R., Kubo, H., Shibata, E., Nakamura, T., 2009. Immobilization of arsenic from novel synthesized scorodite—analysis on solubility and stability. *Mater. Trans.* 50, 321–331. <https://doi.org/10.2320/matertrans.M-MRA2008844>.
- Gadgil, A.J., Roy, J., Addy, S., Das, A., Miller, S., Dutta, A., Debsarkar, A., 2012. Addressing arsenic poisoning in South Asia. *Solutions* 5, 40–45.
- Ghosh, A., Mukhiibi, M., Ela, W., 2004. TCLP underestimates leaching of arsenic from solid residuals under landfill conditions. *Environ. Sci. Technol.* 38, 4677–4682. <https://doi.org/10.1021/es030707w>.
- Ghosh, A., Mukhiibi, M., Sáez, A.E., Ela, W.P., 2006. Leaching of arsenic from granular ferric hydroxide residuals under mature landfill conditions. *Environ. Sci. Technol.* 40, 6070–6075. <https://doi.org/10.1021/es060561b>.
- Glasser, F.P., 1997. Fundamental aspect of cement solidification and stabilization. *J. Hazard. Mater.* 52 (2–3), 151–170.
- Hassan, K.M., Fukushi, K., Turikuzzaman, K., Moniruzzaman, S.M., 2014. Effects of using arsenic-iron sludge wastes in brick making. *Waste Manag.* 34, 1072–1078. <https://doi.org/10.1016/j.wasman.2013.09.022>.
- Jing, C., Korfiatis, G.P., Meng, X., 2003. Immobilization mechanisms of arsenate in Iron hydroxide sludge stabilized with cement. *Environ. Sci. Technol.* 37, 5050–5056. <https://doi.org/10.1021/es021027g>.
- Liang, Y., Min, X., Chai, L., Wang, M., Liyang, W., Pan, Q., Okido, M., 2017. Stabilization of arsenic sludge with mechanochemically modified zero valent iron. *Chemosphere* 168, 1142–1151. <https://doi.org/10.1016/j.chemosphere.2016.10.087>.
- Manceau, A., Fourier, U.J., 1993. Local structure of ferrihydrite and ferroxidite by EXAFS spectroscopy. pp. 165–184.
- Martínez-Cabanas, M., Carro, L., López-García, M., Herrero, R., Barriada, J.L., Sastre de Vicente, M.E., 2015. Achieving sub-10ppb arsenic levels with iron based biomass-silica gel composites. *Chem. Eng. J.* 279, 1–8. <https://doi.org/10.1016/j.cej.2015.04.148>.
- MoEF, 2008. Hazardous wastes (management, handling and transboundary movement) rules. Gov. India Minist. Environ. For. 1–40 <https://doi.org/24the September 2009>.
- MoEFCC, 2016. The hazardous and other wastes (management and transboundary movement) rules. Gov. India Minist. Environ. For. Clim. Change 1–68.
- Möschner, G., Lothenbach, B., Rose, J., Ulrich, A., Figi, R., Kretzschmar, R., 2008. Solubility of Fe-ettringite (Ca₆[Fe(OH)₆]2(SO₄)₃ · 26H₂O). *Geochim. Cosmochim. Acta* 72, 1–18. <https://doi.org/10.1016/j.gca.2007.09.035>.
- Nazari, A.M., Radzinski, R., Ghahreman, A., 2016. Review of arsenic metallurgy: treatment of arsenical minerals and the immobilization of arsenic. *Hydrometallurgy*. <https://doi.org/10.1016/j.hydromet.2016.10.011>.
- Olsen, S.R., Cole, C.V., Watanabe, F.S., Dean, L. a., 1954. Estimation of available phosphorus in soils by extraction with sodium bicarbonate. *USDA Circ.* 939, 1–19. <https://doi.org/10.2307/302397>.
- Paktunc, D., Dutrizac, J., Gertsman, V., 2008. Synthesis and phase transformations involving scorodite, ferric arsenate and arsenical ferrihydrite: Implications for arsenic mobility. *Geochim. Cosmochim. Acta* 72 (11), 2649–2672. <https://doi.org/10.1016/J.GCA.2008.03.012>.
- Patterson, G., 2006. High efficiency ion exchange technology brings arsenic compliance to Baldy Mesa water district. *J. Am. Water Works Assoc.* 98, 26–28.
- Shafiquzzaman, M., Azam, M.S., Nakajima, J., Bari, Q.H., 2010. Arsenic leaching characteristics of the sludges from iron based removal process. *Desalination* 261, 41–45. <https://doi.org/10.1016/j.desal.2010.05.049>.
- Shah, M.H., Shaheen, N., Jaffar, M., Khaliq, A., Tariq, S.R., Manzoor, S., 2006. Spatial variations in selected metal contents and particle size distribution in an urban and rural atmosphere of Islamabad, Pakistan. *J. Environ. Manag.* 78, 128–137. <https://doi.org/10.1016/j.jenvman.2005.04.011>.
- Shrestha, R.R., Shrestha, M.P., Upadhyay, N.P., Pradhan, R., Khadka, R., Maskey, A., Maharjan, M., Tuladhar, S., Dahal, B.M., Shrestha, K., 2003. Groundwater arsenic contamination, its health impact and mitigation program in Nepal. *J. Environ. Sci. Health Part A* 38, 185–200. <https://doi.org/10.1081/ESE-120016888>.
- Singh, T.S., Pant, K.K., 2006. Solidification/stabilization of arsenic containing solid wastes using portland cement, fly ash and polymeric materials. *J. Hazard. Mater.* 131, 29–36. <https://doi.org/10.1016/j.jhazmat.2005.06.046>.
- Stronach, S.A., Walker, N.L., Macphree, D.E., Glasser, F.P., 1997. Original contribution reactions between cement and As (III) oxide: the system CaO-SiO₂-As₂O₃-H₂O AT 25 ° C. *Science* (80-.) 17, 9–13.
- USEPA, 2005. Toxicity Characteristic Leaching Procedure. United States Environ. Prot. Agency SOP: 1831. pp. 1–12.
- USEPA, 2002. Implementation guidance for the arsenic rule drinking water regulations for arsenic and clarifications to compliance and new source contaminants monitoring. United States Environ. Prot. Agency, pp. 83.
- USEPA, 1996. USEPA Method 3050B: ACID DIGESTION OF SEDIMENTS, SLUDGES, AND SOILS. United States Environ. Prot. Agency In SW-846. pp. 1–12.
- van Genuchten, C.M., Addy, S.E.A., Peña, J., Gadgil, A.J., 2012. Removing arsenic from synthetic groundwater with iron electrocoagulation: An Fe and As K-edge EXAFS study. *Environ. Sci. Technol.* 46, 986–994. <https://doi.org/10.1021/es201913a>.
- van Genuchten, C.M., Peña, J., 2016. Antimonate and arsenate speciation on reactive soil minerals studied by differential pair distribution function analysis. *Chem. Geol.* 429, 1–9. <https://doi.org/10.1016/j.chemgeo.2016.03.001>.
- van Genuchten, C.M., Peña, J., Amrose, S.E., Gadgil, A.J., 2014. Structure of Fe(III) precipitates generated by the electrolytic dissolution of Fe(0) in the presence of groundwater ions. *Geochim. Cosmochim. Acta* 127, 285–304. <https://doi.org/10.1016/j.gca.2013.11.044>.
- Vandecasteele, C., Dutré, V., Geysen, D., Wauters, G., 2002. Solidification/stabilisation of arsenic bearing fly ash from the metallurgical industry. *Immobilisation mechanism of arsenic. Waste Manag.* 22, 143–146. [https://doi.org/10.1016/S0956-053X\(01\)00062-9](https://doi.org/10.1016/S0956-053X(01)00062-9).
- Vespa, M., Wieland, E., Dähn, R., Lothenbach, B., 2015. Identification of the thermodynamically stable Fe-containing phase in aged cement pastes. *J. Am. Ceram. Soc.* 98, 2286–2294. <https://doi.org/10.1111/jace.13542>.
- Waychunas, G.A., Rea, B.A., Fuller, C.C., Davis, J.A., 1993. Surface chemistry of ferrihydrite: Part I. EXAFS studies on geometry of coprecipitated and adsorbed arsenate. *Geochim. Cosmochim. Acta* 57, 2251–2269. [https://doi.org/10.1016/0016-7037\(93\)90567-G](https://doi.org/10.1016/0016-7037(93)90567-G).
- Webb, S.M., 2005. SIXPack a graphical user interface for XAS analysis using IFEFIT. *Phys. Scr. T115*, 1011–1014. <https://doi.org/10.1238/Physica.Topical.115a01011>.
- WHO, 2011. Guidelines for drinking-water quality. *World Heal. Organ.* 1, 104–108. [https://doi.org/10.1016/S1462-0758\(00\)00006-6](https://doi.org/10.1016/S1462-0758(00)00006-6).
- WHO, 1996. Guidelines for drinking-water quality - second edition - volume 2 - health criteria and other supporting information. *World Heal. Org.* 2, 1–14.
- Yoshida, T., Yamauchi, H., Fan Sun, G., 2004. Chronic health effects in people exposed to arsenic via the drinking water: Dose-response relationships in review. *Toxicol. Appl. Pharmacol.* 198, 243–252. <https://doi.org/10.1016/j.taap.2003.10.022>.